MONTHLY
WEATHER
REVIEW

VOLUME 92, NUMBER 4

APRIL 1964

THE FINITE AMPLITUDE MOUNTAIN WAVE PROBLEM WITH ENTROPY AS A VERTICAL COORDINATE

T. N. KRISHNAMURTI

Department of Meteorology, University of California, Los Angeles, Calif.

ABSTRACT

The equation for steady two-dimensional mountain waves is expressed in the isentropic coordinates. An elliptic equation for the finite amplitude vertical motion field is solved by a numerical marching scheme in atmospheres with varying shear and stability.

1. INTRODUCTION

Consider a vertical half plane (x, z) bounded below by a mountain on a flat ground. A flow which is uniform and horizontal at $x=-\infty$ upon reaching the mountain undergoes vertical perturbations, and gravity waves are produced. A study of these perturbations has been known as the mountain wave problem.

The problem of steady two-dimensional mountain waves was first systematically treated by Lyra [8]. One could perhaps refer to the earlier contributions in the 1880's, when Rayleigh [14] and Kelvin [7] solved the problem of waves on the free surface of a lake with a corrugated bottom. This class of waves is external to the fluid and has been of great help to meteorologists in various formulations of problems dealing with free surface waves. The other class (Lyra [8]) deals with gravity waves in the interior of the fluid and these are the ones of great interest because they are induced by mountains of a certain scale. Queney's [12] contribution forms an important part of our knowledge of these types of air flow over mountains, because his work deals with more realistic mountain profiles than those of Lyra. Both Lyra and Queney consider the propagation of mountain waves in an isothermal atmosphere with no vertical wind shear. This medium has been investigated for a long time (Bjerknes et al. [2]). In this medium the well-known Brunt-Väisälä frequency separates the acoustic waves from the gravity wave spectrum.

A natural extension to the constant-temperature, constant-wind model was made by Wurtele [19]. He introduced a single-layer model with constant stability and constant wind shear. This analytical model is shown to have an interesting spectrum of free waves.

Scorer [15] was among the first to investigate a two-layer model systematically. Zierep [20] extended this work to obtain solutions for a two-layer model with a troposphere and stratosphere.

The problem of vertical propagation of energy by various types of meteorological waves has been the subject of considerable research in recent years, e.g., Charney and Drazin [3], Eliassen and Palm [5].

Without specifying any particular lower tropospheric energy source, Charney and Drazin investigated the general properties of the atmosphere during different seasons. By defining an index of refraction for the atmosphere as a function of the mean zonal wind and the temperature stratification they derived an equation for wave propagation in the vertical direction. This equation is analogous to the equation that describes the transmission of electromagnetic radiation in heterogeneous media. The choice of a quasi-geostrophic model precludes pure gravity waves and their analysis thus refers to the propagation of

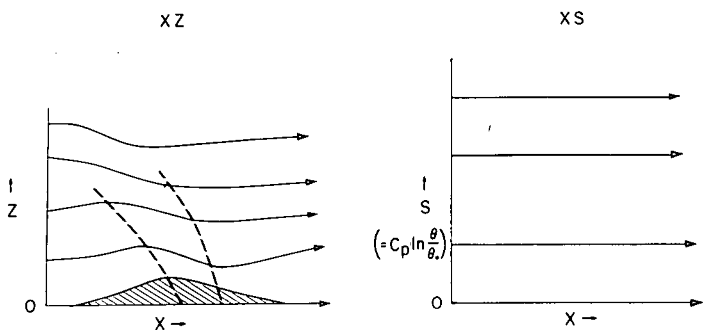

FIGURE 1.—Schematic streamline of a mountain wave problem in the x, z and x, s frames.

energy by long finite-amplitude, planetary-scale disturbances. They found that except for short periods during autumn and spring the atmospheric structure is such that it does not permit vertical energy propagation by these long planetary waves. This is an important result because large amounts of atmospheric energy are found in this scale of motion.

Eliassen and Palm [5] were interested in the problem of vertical energy propagation by gravity waves of small amplitude. Basing the computations on Scorer's [15] solution for the linearized two-dimensional inviscid flow of air over mountains, they derived expressions for reflection coefficients in two- and three-layer models. Calculations based on some wintertime data showed that energy can be transmitted from the troposphere into the high stratosphere and ionosphere by these small-amplitude gravity waves. These results supported suggestions made by Hines [6] that the turbulence at very high levels (80–100 km.) is maintained by energy of gravity waves from the lower troposphere.

Palm and Foldvik [11] looked into the propagation of mountain wave energy to very great heights. They examined individual atmospheric soundings and postulated simplified models to explain the presence of waves in the high stratosphere.

The steady two-dimensional mountain wave in an inviscid atmosphere is described by an elliptic second-order linear differential equation for the perturbation vertical velocity. All the aforementioned references deal with solutions of this differential equation as a boundary value problem. Some of the obvious shortcomings of this approach have been listed by Queney et al. [13]. It might be worth mentioning here that the most important of these are perhaps the choice of finite sized mountains (height 1 km. or over) and the applying of linear theory to understand the structure of waves. Other difficulties lie in the choice of boundary conditions and in specifying the uniqueness of the problem.

In order to overcome the first of these difficulties we propose a reformulation of the mountain wave problem with entropy as a vertical coordinate. We shall show that this yields an elliptic differential equation for the vertical velocity where the mountain surface is treated as a coordinate surface.

Schematically, figure 1 illustrates the two coordinates x,z and x,s, where s stands for entropy. In the x,s system the height of the isentropic surface z is a dependent variable. One can justify a finite amplitude mountain wave problem in the x,s frame by applying boundary conditions along $s=0$. On the contrary for a finite amplitude mountain wave it seems incorrect to apply the boundary conditions at $z=0$ in the x,z frame. We propose to examine a nonlinear mountain wave theory in the x,s frame.

Further we shall be guided by a numerical approach, in which we explicitly introduce a marching scheme for resolving the uniqueness of the problem. The numerical approach has the advantage that one can introduce any arbitrarily shaped mountain. In this connection it might be worth noting that Wallington [18] suggested how one could partition any mountain into a number of idealized step profiles of ridges of different height, width, and phase. Our aim is to bring in a more continuous topography.

2. THE FORMULATION OF THE LINEAR PROBLEM IN THE x,z FRAME

The equation of motion along the x and z directions, the equations of continuity, the adiabatic relation, and the physical equation for a perfect gas may be written in the form

$$u\frac{\partial u}{\partial x}+w\frac{\partial u}{\partial z}=-\frac{1}{\rho}\frac{\partial p}{\partial x} \tag{1}$$

$$u\frac{\partial w}{\partial x}+w\frac{\partial w}{\partial z}=-\frac{1}{\rho}\frac{\partial p}{\partial z}-g \tag{2}$$

$$u\frac{\partial \rho}{\partial x}+w\frac{\partial \rho}{\partial z}=-\rho\left(\frac{\partial u}{\partial x}+\frac{\partial w}{\partial z}\right) \tag{3}$$

$$u\frac{\partial T}{\partial x}+w\frac{\partial T}{\partial z}=-\frac{1}{\rho c_p}\left(u\frac{\partial p}{\partial x}+w\frac{\partial p}{\partial z}\right) \tag{4}$$

$$p=RT\rho \tag{5}$$

where the symbols have the following meaning:

u=component of velocity of air along the x-axis
w=component of velocity of air along the z-axis
p=pressure
c_p,c_v=specific heat of air at constant pressure and volume
ρ=density
T=temperature
R=universal gas constant
g=acceleration of gravity

By linearizing equations (1) through (5) one can formulate the boundary value problem for the vertical velocity and introduce mountain effects as the boundary condition. This is essentially the approach that was followed by Lyra [8] and Queney [12]. Solutions for the other four variables (u,p,T,ρ) are obtained by quadratures as shown, for instance, by Zierep [20].

We shall introduce mean and perturbation quantities in the conventional manner. Let

$$\begin{array}{rcll} & & \text{Mean} \quad \text{Perturbation} & \\ u & = & \overline{U}(z)+u'(x,z) & (6) \\ w & = & w'(x,z) & (7) \\ T & = & \overline{T}(z)+T'(x,z) & (8) \\ \rho & = & \bar{\rho}(z)+\rho'(x,z) & (9) \\ p & = & \bar{p}(z)+p'(x,z) & (10) \end{array}$$

The mean state is uniquely identified by an arbitrary wind distribution $\overline{U}(z)$ and a hydrostatic atmosphere

$$g=-\frac{1}{\bar{\rho}}\frac{\partial \bar{p}}{\partial z} \tag{11}$$

Through a very lengthy process of elimination of the nonlinear terms one obtains a second-order linear differential equation for the perturbation vertical velocity field w (Queney et al. [13]).

$$\overline{M}\frac{\partial^2 w}{\partial x^2}+\frac{\partial^2 w}{\partial z^2}-\overline{S}\frac{\partial w}{\partial z}+\left(\frac{\bar{\beta}g}{\overline{U}^2}+\frac{\overline{S}\frac{d\overline{U}}{dz}}{\overline{U}}-\frac{\frac{d^2\overline{U}}{dz^2}}{\overline{U}}\right)w=0 \tag{12}$$

where

$$\overline{M}=1-\frac{\overline{U}^2}{\overline{C}^2}$$

$$\overline{S}=\frac{d}{dz}\ln\bar{\rho}+\frac{1}{\overline{M}}\frac{d\overline{M}}{dz}$$

$$\bar{\beta}=\frac{d}{dz}\ln\bar{\theta}+\frac{1}{\overline{M}}\frac{d\overline{M}}{dz}$$

and

$$\bar{\theta}=\overline{T}\left(\frac{p}{p_o}\right)^{-R/c_p}$$

In equation (12) $\overline{M}$ represents a departure of the square of the Mach number from unity and in the atmosphere is known to be positive. Hence, equation (12) is an elliptic differential equation for the vertical velocity w; $\overline{S}$ and $\bar{\beta}$ are respectively related to the density and temperature stratifications in the vertical. $\bar{\theta}$ is the potential temperature.

A canonical form of equation (12) may be obtained by introducing a new variable,

$$w^{(1)}=we^{-\int(\overline{S}/2)dz} \tag{13}$$

This results in the equation

$$\nabla_z^2 w^{(1)}+F(z)w^{(1)}=0 \tag{14}$$

where

$$\nabla_z^2\equiv\overline{M}\frac{\partial^2}{\partial x^2}+\frac{\partial^2}{\partial z^2}$$

and

$$F(z)=\frac{\bar{\beta}g}{\overline{U}^2}+\frac{\overline{S}\frac{dU}{dz}}{\overline{U}}-\frac{1}{4}\overline{S}^2+\frac{1}{2}\frac{d\overline{S}}{dz}-\frac{1}{\overline{U}}\frac{d^2\overline{U}}{dz^2}$$

Equation (14) is a homogeneous wave equation.

The two-dimensional mountain wave problem consists in obtaining formal solutions of equation (14) for suitably defined boundary conditions. This theory has been the basis of most of the earlier formulations of the two-dimensional mountain wave problem. Refer to Queney et al. [13].

3. THE FINITE AMPLITUDE MOUNTAIN WAVE PROBLEM IN THE x,s FRAME

The following two relations are well known coordinate transforms that relate derivates in the x,s and x,z frames.

$$\left.\frac{\partial Q}{\partial x}\right)_s=\left.\frac{\partial Q}{\partial x}\right)_z+\left.\frac{\partial Q}{\partial z}\frac{\partial z}{\partial x}\right)_s \tag{15}$$

$$\frac{\partial Q}{\partial s}=\frac{\partial Q}{\partial z}\frac{\partial z}{\partial s} \tag{16}$$

By use of these relations and through a lengthy algebraic manipulation we may rewrite equations (1) through (5) into the following set of three nonlinear differential equations for the variables u, z, and T.

$$u\frac{\partial u}{\partial x}\frac{\partial z}{\partial s}+c_p\frac{\partial T}{\partial x}\frac{\partial z}{\partial s}-\frac{\partial z}{\partial x}\left(c_p\frac{\partial T}{\partial s}-T\right)=0 \tag{17}$$

$$u\frac{\partial z}{\partial s}\frac{\partial}{\partial x}\left(u\frac{\partial z}{\partial x}\right)+c_p\frac{\partial T}{\partial s}-T+g\frac{\partial z}{\partial s}=0 \tag{18}$$

$$\frac{c_v}{RT}\frac{\partial T}{\partial x}\left(u\frac{\partial z}{\partial s}\right)+\frac{\partial}{\partial x}\left(u\frac{\partial z}{\partial s}\right)=0 \tag{19}$$

Equations (17) and (18) are the equations of motion along the x and s (the vertical) coordinates. Equation (19) is the transformed adiabatic relation. For this system x and s are the independent coordinates; z represents a dependent variable, the height of the isentropic surface s at any point x.

It can now be shown quite easily that the linearized system obtained from equations (17), (18), and (19) yields an elliptic equation for the vertical velocity that is very similar to equation (12).

For this purpose mean and perturbation variables are introduced as follows:

$$\begin{array}{rcllll} & & \text{Mean} & & \text{Perturbation} & \\ u & = & U(s) & + & u'(x,s) & (20) \\ z & = & H(s) & + & z'(x,s) & (21) \\ T & = & \mathcal{T}(s) & + & T'(x,s) & (22) \end{array}$$

Where $U(s)$, $H(s)$, and $T(s)$ respectively are the mean values of the horizontal wind, height, and temperature on an isentropic surface s.

It is further assumed that the mean field is in hydrostatic equilibrium, or,

$$\frac{dH}{ds}=\frac{1}{g}\left(T-c_p\frac{dT}{ds}\right) \tag{23}$$

We may separate the linear and the nonlinear parts of equations (17) through (19) and rewrite them in the form

$$U\left(\frac{\partial u}{\partial x}\right)+c_p\left(\frac{\partial T}{\partial x}\right)+g\left(\frac{\partial z}{\partial x}\right)=N_1 \tag{24}$$

$$U^2\frac{\partial H}{\partial s}\left(\frac{\partial^2 z}{\partial x^2}\right)+g\left(\frac{\partial z}{\partial s}\right)+c_p\left(\frac{\partial T}{\partial s}-\frac{T}{c_p}\right)=N_2 \tag{25}$$

$$\frac{c_vU}{RT}\frac{\partial H}{\partial s}\left(\frac{\partial T}{\partial x}\right)+\frac{\partial H}{\partial s}\left(\frac{\partial u}{\partial x}\right)+U\frac{\partial^2 z}{\partial x\partial s}=N_3 \tag{26}$$

where N_1, N_2, and N_3 are the nonlinear terms.

In order to obtain a differential equation for the vertical velocity in the x,s frame we may treat equations (24) and (26) as two simultaneous equations for the variables $\partial T/\partial x$ and $\partial u/\partial x$. On solving these simultaneous equations we may express (25) as functions of the height (z) field and the nonlinear terms. We may then differentiate equation (25) with respect to x and substitute for $\partial u/\partial x$ and $\partial T/\partial x$ and obtain a differential equation for the slope of the isentropic surfaces. This yields

$$F_1\frac{\partial^2}{\partial x^2}\left(\frac{\partial z}{\partial x}\right)_s+F_2\frac{\partial}{\partial s}\left(\frac{\partial z}{\partial x}\right)_s+F_3\frac{\partial^2}{\partial s^2}\left(\frac{\partial z}{\partial x}\right)_s+F_4\left(\frac{\partial z}{\partial x}\right)_s+N_4=0 \tag{27}$$

where F_1, F_2, F_3, and F_4 are functions of x and s and are determined by the temperature and wind stratifications of the mean flow. N_4 is the nonlinear term.

$$F_1=U^2\frac{\partial H}{\partial s} \tag{28}$$

$$F_2=g+c_p\left[\frac{g}{\frac{U^2c_v}{RT}-c_p}-\frac{\partial}{\partial s}\frac{U^2}{\left(\frac{U^2c_v}{RT}\frac{\partial H}{\partial s}-c_p\frac{\partial H}{\partial s}\right)}\right]+\frac{U^2}{\frac{U^2c_v}{RT}\frac{\partial H}{\partial s}-c_p\frac{\partial H}{\partial s}} \tag{29}$$

$$F_3=\frac{c_pU^2}{\frac{\partial H}{\partial s}\left(c_p-\frac{U^2c_v}{RT}\right)} \tag{30}$$

$$F_4=c_p\left[\frac{\partial}{\partial s}\frac{g}{\frac{U^2c_v}{RT}-c_p}\right]-\frac{g}{\frac{U^2c_v}{RT}-c_p} \tag{31}$$

Equation (27) is the differential equation for the vertical velocity in the x,s frame. It is easy to see that $U(\partial z/\partial x)_s$ would be the vertical velocity for the linear problem.

The finite amplitude mountain wave problem consists in solving equation (27) as a boundary value problem, by some iterative scheme. The solution of the linear problem in the x, s frame would be obtained for $N_4=0$.

In this paper we shall utilize the well-known Perturbation-Iteration scheme for the finite amplitude expansion. We start with $N_4=0$ and build successively the nonlinear solutions by constructing the field of N_4.

4. A COMPARISON OF THE TWO COORDINATE SYSTEMS

The linear differential equations for the vertical velocity in the two coordinates appear to have complicated coefficients; these depend on the stability and shear parameters. In order to compare these equations it would be best to examine first a simple model and then perhaps we can make some general comments.

Consider an isothermal atmosphere having no vertical wind shear for the mean state. We may rewrite equations (12) and (27), the respective equations for the vertical velocity in the x,z and x,s frames, as:

$$\overline{M}\frac{\partial^2 w}{\partial x^2}+\frac{\partial^2 w}{\partial z^2}-\left(\frac{g}{R\overline{T}}\right)\frac{\partial w}{\partial z}+\left(\frac{g^2}{c_p\overline{T}\overline{U}^2}\right)w=0 \tag{32}$$

$$\left\{\frac{\left(\frac{\partial H}{\partial s}\right)^2\left(c_p-\frac{\overline{U}^2c_v}{RT}\right)}{c_p}\right\}\frac{\partial^2 P}{\partial x^2}+\frac{\partial^2 P}{\partial s^2}-\left(\frac{1}{R}\right)\frac{\partial P}{\partial s}+\left(\frac{g\frac{\partial H}{\partial s}}{c_pU^2}\right)P=0 \tag{33}$$

where $P=(\partial z/\partial x)_s$ is the slope of the isentropic surfaces.

The canonical forms of (32) and (33) may be written in the usual manner.

$$\nabla_z^2w^{(1)}+\frac{g^2}{\overline{T}^2}\left(\frac{\overline{T}}{c_p\overline{U}^2}-\frac{1}{4R^2}\right)w^{(1)}=0 \tag{34}$$

$$\nabla_s^2P^{(1)}+\left(\frac{T}{c_pU^2}-\frac{1}{4R^2}\right)P^{(1)}=0 \tag{35}$$

where

$$P^{(1)}=Pe^{-\int(1/R)ds},\quad \nabla_s^2\equiv\left\{\left(\frac{\partial H}{\partial s}\right)^2\frac{\left(c_p-\frac{U^2c_v}{RT}\right)}{c_p}\right\}\frac{\partial^2}{\partial x^2}+\frac{\partial^2}{\partial s^2}$$

Equations (34) and (35) appear to be very similar except we note that if we were to make a formal coordinate transformation at this stage from the x,s to the x,z frame, then

$$\nabla_z^2w\neq\nabla_s^2w$$

In this context perhaps it might be worth examining figure 2 which outlines the correspondence of the two systems.

This figure shows that starting with the complete nonlinear equation in the two frames $xs^{(N)}$ and $xz^{(N)}$, on linearizing in their respective frames one obtains $xs^{(L)}$ and $xz^{(L)}$ that are not identical. If we make coordinate transformations from the s to z system, or from the z to s system, we obtain second nonlinear systems $xz^{(N2)}$ and $xs^{(N2)}$ which on linearization yield $xz^{(L)}$ and $xs^{(L)}$.

The results of figure 2 have been shown by the author to be true for the simple atmospheric model considered in this section. But there is reason to believe that this is generally true.

5. ON THE UNIQUENESS OF THE PROBLEM

The two-dimensional mountain wave problem has been recognized, since the works of Lords Rayleigh [14] and Kelvin [7], as one that has several eigensolutions. These eigensolutions can always be added to the solutions of the wave equation for specific boundary conditions. In order to render the problem unique, Rayleigh introduced friction terms that were proportional to the velocity. These have since become known as the "Rayleigh friction" terms. Then by letting friction tend to zero in the solutions he was able to obtain the so-called downstream mode in a lee wave problem; the upstream mode was removed. Kelvin rendered the problem unique by asking for the mode which has *no mountain wave* effect very far *upstream* from the mountain. We shall show in the following analysis of the numerical finite amplitude problem that the finite difference form of the equation can be formulated to produce unique solutions.

In particular we shall illustrate a numerical analogue for the Kelvin monotony condition that will consist in solving the boundary value elliptic equation by a marching scheme.

It is pertinent, perhaps, to recall here that the Sommerfeld [16], [17] radiation conditions also render the problem unique, where the upstream mode is discarded from considerations of energetics, there being no physical wave energy source at the top of the atmosphere. Some initial value problems of the two-dimensional mountain wave also are known to have unique solutions. References to these works may be found in Queney et al. [13].

6. THE LYRA PROBLEM IN THE TWO COORDINATES

We may, for instance, examine the problem that Lyra [8] considered in 1940. He was interested in solution of the linear wave equation (34) in the x,z frame. A narrow rectangular hill (fig. 3) constitutes the mountain. The boundary conditions for the problem are:

$$
\begin{aligned}
w^{(1)}&=0 &,\quad & x=\pm\infty\\
w^{(1)}&=\overline{U}(\partial h/\partial x) &,\quad & z=0\\
w^{(1)}&=0 &,\quad & z=\infty
\end{aligned}
$$

where h is the height of the mountain above $z=0$. This

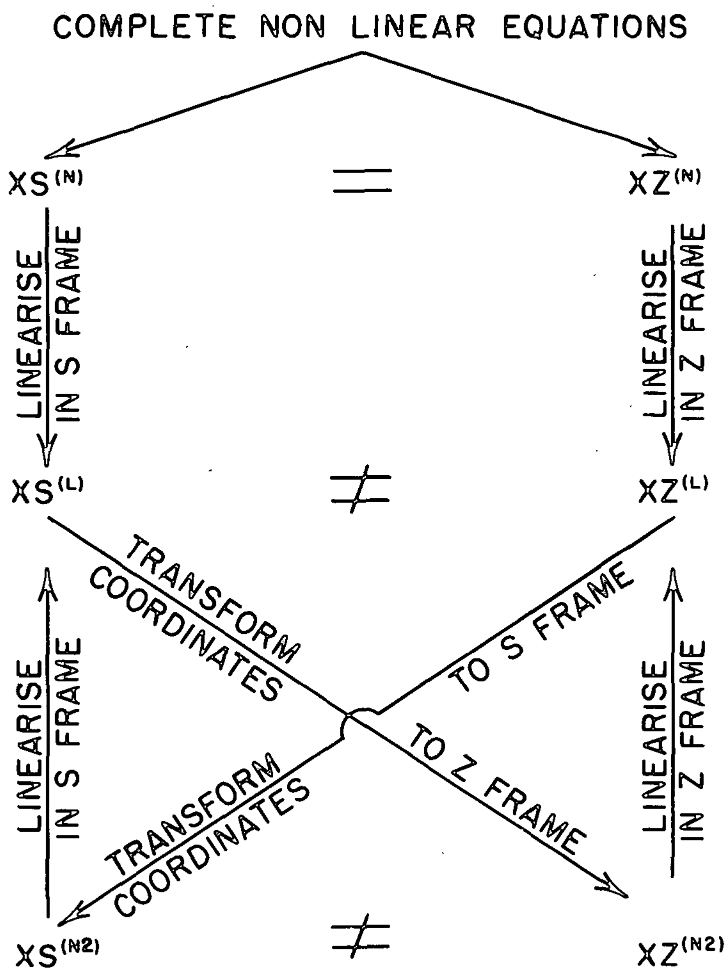

FIGURE 2.—Depicts the coordinate transformation and the equivalence of the equations in the linear and nonlinear frames.

problem has several eigensolutions (or, the free waves) and Lyra was able to obtain uniqueness by invoking the conditions stated in the previous section. For the specific rectangular obstacle located at the origin $x=z=0$ of height h and limiting area F he obtained the following solution:

$$
w=-\frac{\pi\overline{U}F}{\lambda_z}z\,e^{gz/2R\overline{T}}\frac{\partial}{\partial x}\left[\frac{N_1\left(\frac{2\pi}{\lambda_z}\sqrt{x^2+z^2}\right)}{\sqrt{x^2+z^2}}+\frac{xJ_2\left(\frac{2\pi}{\lambda_z}\sqrt{x^2+z^2}\right)}{x^2+z^2}\right] \tag{36}
$$

where

$$
\lambda_z=\frac{1}{K_z}=\frac{\overline{T}}{g}\sqrt{\frac{1}{\frac{\overline{T}}{c_p\overline{U}^2}-\frac{1}{4R^2}}}
$$

J_2 is the Bessel function of the first kind and of order 2; N_1 is the Bessel function of the second kind.

We may seek solutions of the wave equation (35) in the x,s frame in a similar manner. As boundary conditions we may consider:

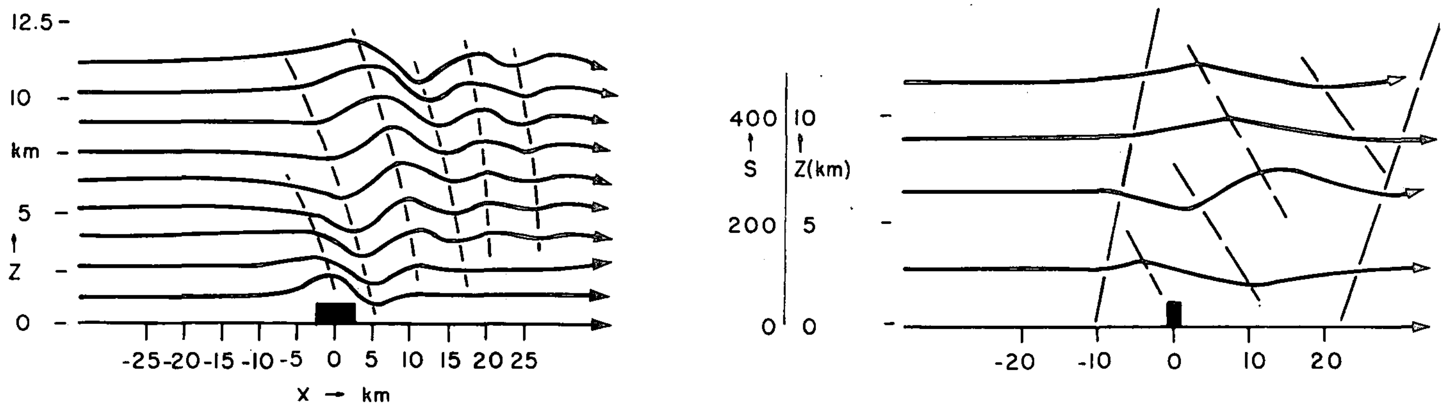

FIGURE 3.—A comparison of the Lyra solution (left) for a rectangular hill with the numerical solution (right) for a hill 1 km. high at one grid point.

$$P^{(1)}=0 \quad , \quad s=\infty$$

$$P^{(1)}=\left.\frac{\partial h}{\partial x}\right)_{s=0} \quad , \quad s=0$$

$$P^{(1)}=0 \quad , \quad x=\pm\infty$$

We can show that the corresponding solution is:

$$P=\left.\frac{\partial z}{\partial x}\right)_s=-\frac{\pi F}{\lambda_s}se^{s/2R}\frac{\partial}{\partial x}\cdot\left[\frac{N_1\left(\frac{2\pi}{\lambda_s}\sqrt{x^2+s^2}\right)}{\sqrt{x^2+s^2}}+\frac{xJ_2\left(\frac{2\pi}{\lambda_s}\sqrt{x^2+s^2}\right)}{x^2+s^2}\right] \tag{37}$$

where

$$\lambda_s=\frac{1}{k_s}=\sqrt{\frac{1}{\frac{T}{c_pU^2}-\frac{1}{4R^2}}}$$

A casual examination of the analytical forms of the solution (36) and (37) in the two frames may lead one to believe that they are identical. There is however the interesting difference as already mentioned in figure 2.

In the x,s system the vertical velocity is geometrically placed at the correct position by virtue of the boundary condition. This makes a systematic difference at all higher levels. The difference in magnitudes of the vertical velocity at the two corresponding points is of the order introduced by the coordinate transformation, figure 2. This can be very large in a typical case.

Meteorologists have now recognised the usefulness of a so-called σ-coordinate. It has the property that $\sigma=1$ is the earth's surface with its topography. It seems to the author that the x,s system is the better coordinate for investigation of mountain waves in an adiabatic atmosphere. The $s=0$ surface is identical to the $\sigma=1$ surface.

7. THE NUMERICAL PROCEDURE

The basic equations of the problem are the elliptic second-order differential equation (27) for the slope P of the isentropic lines and the two equations that relate the temperature T and the horizontal wind speed u to the slope P. These equations may be written respectively as:

$$F_1\frac{\partial^2 P}{\partial x^2}+F_2\frac{\partial P}{\partial s}+F_3\frac{\partial^2 P}{\partial s^2}+F_4P+N_4=0 \tag{38}$$

$$\frac{\partial T}{\partial x}=A_1P+A_2\frac{\partial P}{\partial s}+N_5 \tag{39}$$

$$\frac{\partial u}{\partial x}=B_1P+B_2\frac{\partial P}{\partial s}+N_6 \tag{40}$$

The coefficients F_1, F_2, F_3, F_4, A_1, A_2, B_1, and B_2 are known functions of the mean field.

The suggested iterative scheme is initiated by setting the nonlinear terms $N_4=N_5=N_6=0$.

In a numerical formulation of the problem we are confronted with several problems: (*i*) order of solving the equations, (ii) proper boundary condition for resolving uniqueness, (iii) stable computational scheme to establish convergence of the nonlinear phase.

The order appears to be simple; one could solve for P, T, and u respectively in the order of the three equations.

We propose the following boundary conditions for this problem:

$$x=0 \quad P=0 \tag{41}$$

$$x=\Delta x \quad P=0 \tag{42}$$

$$s=0 \quad P=\left.\frac{\partial z}{\partial x}\right)_{s=0}, \quad \left.\frac{\partial z}{\partial x}\right)_{s=0}=\text{ACTUAL MOUNTAIN SLOPE} \tag{43}$$

$s=s_\infty$ $P=0$ At great heights $s=s_\infty$ no mountain wave exists. (44)

In previous linear studies the vertical velocity at the lower boundaries is simply given by,

$$W=\overline{U}_{z=0}\frac{\partial h}{\partial x}$$

similar to what was stated in the Lyra problem. The procedure outlined in this paper yields,

$$W=(\overline{U}+u)_{z=0}\frac{\partial h}{\partial x}$$

at the lower boundary and hence horizontal variation of the surface wind is possible in this nonlinear lower boundary condition. In this aspect this approach may be considered an improvement over the previous studies.

The first two boundary conditions along $x=0$ and $x=\Delta x$ satisfy the Kelvin monotony condition that there be no wave far upstream from the mountain. The finite difference analog of the linear differential equation (38), $N_4=0$, shows that if $P=0$ at two adjacent lines $x=0$ and Δx then for $\partial z/\partial x)_{s=0}=0$ the solution is $P=0$ everywhere. This assures that in the region upstream from the mountain ($x>0$) there will be no wave. This particular choice of boundary conditions renders it into a marching problem similar to what is normally done for the well known hyperbolic wave equation in physics. The marching problem must satisfy computational stability criteria. A simple comparison with the wave equation suggests that the choice of Δx must satisfy the relation:

$$\Delta x<\Delta s\sqrt{|-F_1/F_3|}$$

It is not frequent that one finds an elliptic differential equation solved by a marching scheme. This problem has imaginary characteristics $-F_1/F_3<0$, and there is no formal computational stability criterion.

According to Morse and Fishbach [10], an elliptic differential equation may be treated as a hyperbolic wave equation only if certain stringent conditions are met. These are that P and $\partial P/\partial x$ at the initial coordinate line, $x=0$.

An examination of figure 4 will illustrate the uniqueness of the numerical solution. The difference equation,

$$F_1(J)\frac{P(I+1,J)+P(I-1,J)-2P(I,J)}{\Delta x^2}+F_2(J)\frac{P(I,J+1)-P(I,J-1)}{2\Delta s}+F_3(J)\frac{P(I,J+1)+P(I,J-1)-2P(I,J)}{\Delta s^2}+F_4(J)P(I,J)+N_4(I,J)=0 \quad (45)$$

may be written for the marching phase as:

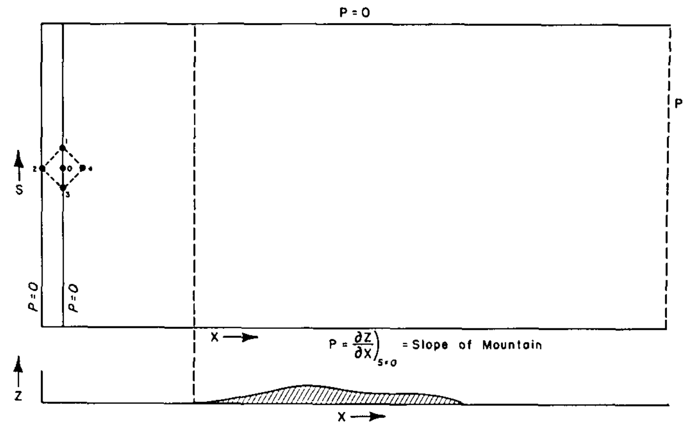

FIGURE 4.—Diagram illustrates the numerical marching scheme for a mountain of any shape (below). Two lines on left $P=0$, initiate the calculation. P at point 4 is determined by values at 0, 1, 2, and 3. Rest described in text.

$$P(I+1,J)=2P(I,J)-P(I-1,J)-\Big[F_2(J)\{P(I,J+1)-P(I,J-1)\}/2\Delta s+F_3(J)\left\{\frac{P(I,J+1)+P(I,J-1)-2P(I,J)}{\Delta s^2}\right\}+F_4(J)P(I,J)+N_4(I,J)\Big]\frac{\Delta x^2}{F_1(J)} \quad (46)$$

If we were to find a computationally stable marching step Δx and integrate from left to right as illustrated in figure 4, then the set of numbers $P^*(L, x)$ far downstream at $x=L$ possesses the following property:

$P^*(L, s)$ is a unique set of numbers consistent with $P=0$ upstream from dashed line. This uniqueness can be further illustrated by stating that: If we were to solve next a boundary value problem by prescribing

$$\begin{array}{lll} P=0 & \text{at} & x=0 \\ P=P^* & & x=L \\ P=0 & & s=s_\infty \\ P=\left.\frac{\partial z}{\partial x}\right)_{s=0} & & s=0 \end{array}$$

then P^* is the only downstream boundary set that would yield $P=0$ left of the dashed line. The argument presented here follows from the properties of the linear difference equation.

The marching scheme may be looked upon as a device for search of the proper downstream boundary conditions for the mountain wave problem. When the downstream boundary condition has been determined by the marching scheme, it may be used to solve the elliptic mountain wave equation by a relaxation procedure. The resulting numbers in the region $0<x<L$, $0<s<s_\infty$ will be identical

for the marching and the relaxation procedures. We find that at the same time the marching scheme exactly satisfies the Kelvin monotony condition.

A comment on the choice of the upper boundary condition at $s=s_\infty$ is perhaps necessary here.

In Lyra and Queney problems the corresponding boundary condition is that at $s=s_\infty$,

$$\tfrac{1}{2}\overline{\rho w^2}=0$$

This boundary condition precludes unbounded energy at great heights; however the vertical velocity w does take on very large values. In a numerical approach large values of p at $s=s_\infty$ makes it very difficult to find a computational scheme that will make the nonlinear phase converge. We have assumed that there be no wave at $s=s_\infty$, (where $s_\infty \approx 100$ km. height).

This condition may be looked upon as that of putting a rigid top on the atmosphere. This is not serious because the wave activity may be expected to die out at these heights in most situations. One might wonder about reflection of energy from the top and thus find it difficult to compare the numerical solutions with Lyra type problems. This is however not the case because the marching scheme produces non-zero numbers essentially from the mountain and up, and the problem of reflection may be only important far downstream, an area we shall not be interested in here.

Support for the proposed use of the upper boundary condition is also given by Corby and Sawyer [4]. They found that the rigid upper boundary exerts little influence on the relatively small gravity waves.

When the boundary condition was raised in their problem to $z=\infty$ the solution approached that given by Queney.

The foregoing arguments for the uniqueness and the computational stability criterion apply for the linear difference equation. We propose to introduce the nonlinear phase by successively generating N_4, N_5, and N_6 through calculations. The nonlinear problem is solved through the following steps:

(i) Solve for P from the linear difference equation ($N_4=0$)

(ii) Solve for u and T from the linear equation by quadratures ($N_5=N_6=0$)

(iii) Generate magnitudes of N_4, N_5, and N_6 from the linear solutions for P, u, and T

(iv) Solve for P from the nonlinear difference equation (N_4 from (iii))

(v) Solve for u and T from the nonlinear equation by quadratures (N_5 and N_6 from (iii))

(vi) Repeat steps (iii), (iv), and (v) until the magnitudes of P, u, T, N_4, N_5, and N_6 converge to acceptable limits of tolerance.

We have tacitly assumed that the steps would produce a converging solution. This is found to be true only in some cases that we shall present here. It might perhaps be pertinent to state here a class of calculations that invariably diverges when we pursue the type of procedure stated above. This occurs when one solves for P by a relaxation or a matrix inversion procedure assuming a known value of $P^*=0$, for instance, at the downstream end. The perturbation energy in this class of problems is confined to a finite area $0\leq x\leq L$ and the iteration procedure yields rather large values for N_4, N_5, and N_6 and the scheme fails. The marching scheme determines P^*, and at $x=L$ there is an open boundary; a large amount of wave energy thus flows out of the region $0\leq x\leq L$, and the iteration scheme yields small magnitudes for N_4, N_5, and N_6. There have been some cases when the marching scheme produced unbounded solutions; there is perhaps some parameter like the Richardson number of the mean flow that controls the stability of the nonlinear iteration scheme. This question will remain unanswered in this paper.

8. SOME RESULTS OF THE NUMERICAL CALCULATIONS

We have used the following constants and units

$\Delta s=200$ m.^{2} sec.$^{-2}$ deg.$^{-1}$

$c_p=1000$ m.^{2} sec.$^{-2}$ deg.$^{-1}$

$s_\infty=4000$ m.^{2} sec.$^{-2}$ deg.$^{-1}$, corresponds to a top around 100 km.

$\Delta x=\Delta s\sqrt{|-F_1/F_3|}$ varies from case to case (20 m. in some calculations)

$L=200$ km.

$\epsilon=c_v/R\equiv 2.46$

$g=9.81$ m. sec.$^{-2}$

ISOTHERMAL ATMOSPHERE WITH NO VERTICAL WIND SHEAR

We propose a problem similar to that of Lyra, where mean temperature $\mathcal{T}=250°$A; mean wind $U=20$ m. sec.$^{-1}$; a mountain of height $h=1$ km. is placed at a single grid point, in this case at $x=x_0=100$ km. from origin. Through finite differences this produces the following boundary condition on P

$$(x_0+\Delta x)\leq x\leq L \qquad P=0$$

$$0\leq x<(x_0-\Delta x) \qquad P=0$$

$$x=x_0\mp\Delta x \qquad P=\pm U\frac{h}{2\Delta x}$$

$$x=x_0 \qquad P=0$$

Through these boundary conditions we can simulate a numerical problem somewhat analogous to the continuous problem of Lyra.

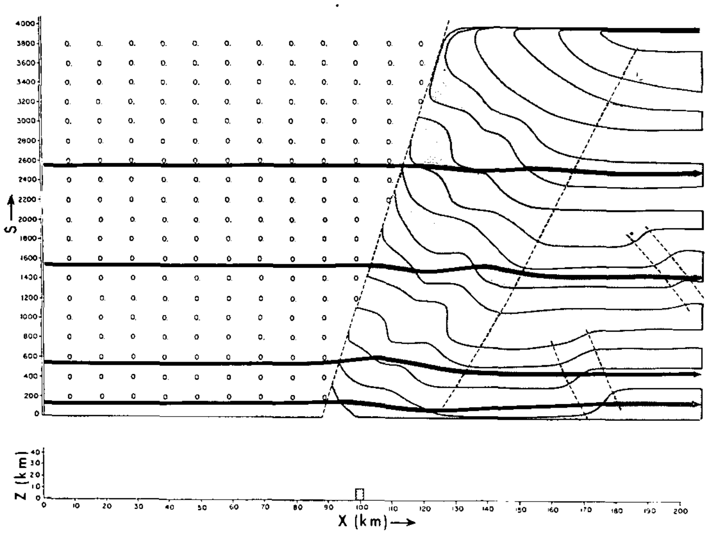

FIGURE 5.—Linear solution for a step mountain 1 km. high. Slopes of streamlines (shown by zeros on left, stippled and clear to the right). The two dashed lines enclose region of maximum wave energy. Heavy dark lines are a few streamlines.

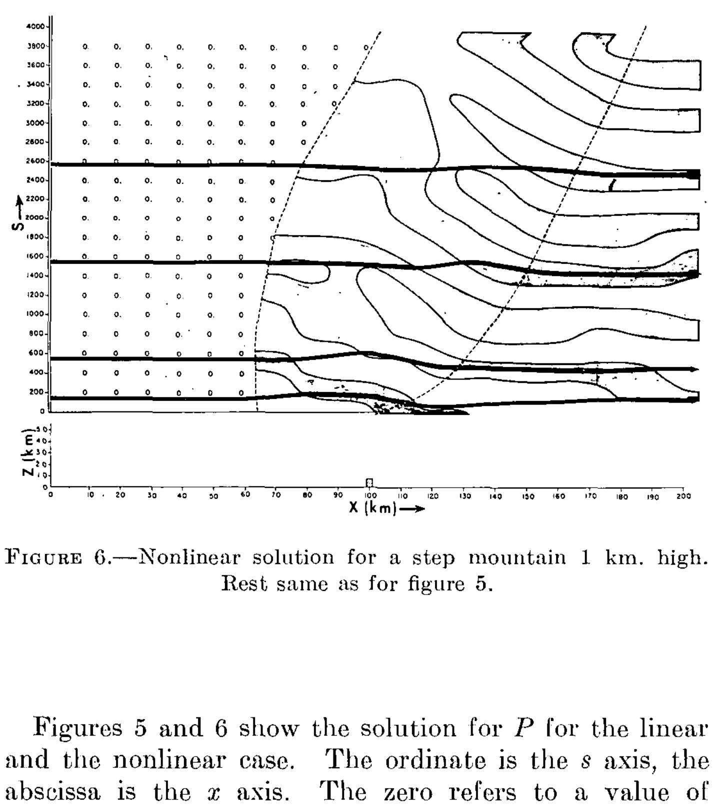

FIGURE 6.—Nonlinear solution for a step mountain 1 km. high. Rest same as for figure 5.

Figures 5 and 6 show the solution for P for the linear and the nonlinear case. The ordinate is the s axis, the abscissa is the x axis. The zero refers to a value of $P(=0)$. In the stippled area P is negative and alternately there are regions $P>0$. The streamline geometry can be inferred from this configuration of P, the slope. In the region where $P=0$ the streamlines are exactly horizontal; the streamlines rise and fall in the clear and stippled region as shown, indicating waves. The two primary dashed lines confine the region of maximum wave energy. There are two secondary regions also

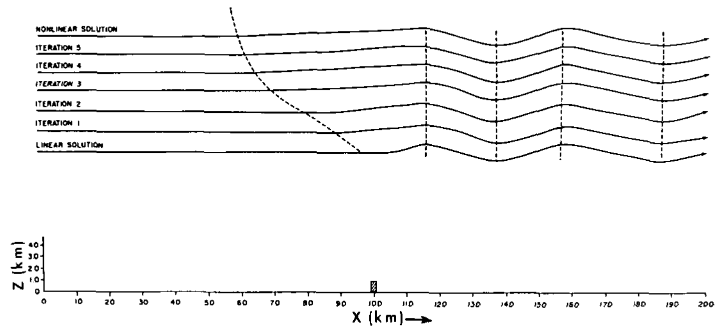

FIGURE 7.—Comparison of the streamline ($s=1800$) for various iterations. Narrow hill of 1 km. at one grid point.

confined between dashed lines that contain small amounts of wave energy to the right of the primary mode.

The magnitude of P (not indicated in the figures) decreases very rapidly with height; starting from $P=10^{-2}$ at $s=0$, it reaches values of the order $P=10^{-20}$ in the upper region $s=1800$. The amount of wave energy in the upper part of the perturbed region is very small.

The nonlinear solution differs from the linear solution in only one major respect. In the region $x<(x_0-\Delta x)$ there is no mountain wave, as one should expect from the linear difference equation. The wave action recedes upstream in the nonlinear phase.

To illustrate this feature of the nonlinear calculation an individual streamline for various iterations is illustrated in figure 7. The positions of the major troughs and ridges of the particular streamline ($s=1800$) are unaltered; the first dashed line to the left shows the farthest point upstream where P is non-zero. In most of the grid points the calculations converged after six iterations, to a reasonable tolerance.

Figure 7 shows little or no change in the geometry of the troughs and ridges when the nonlinear terms are included in the linear solution. This appears to be in contrast to the nonlinear solution of Palm and Foldvik [11] who found that the troughs tended to flatten and ridges or crests tended to sharpen with the inclusion of the nonlinear influences. Palm and Foldvik attribute these to a possible connection with the shear of the mean wind. Figure 7 represents the condition for an atmosphere with no mean vertical wind shear and could thus explain the differences in the results.

Figure 8 shows the convergence at individual grid points of P and N_4 (the nonlinear inhomogenous term). The ordinate shows the function P and N_4 plotted against the iteration number.

It appears from this set of calculations that the nonlinear terms in the x,s frame are very small. This need not be so in the x,z frame.

In the right of figure 3 we have presented this numerical solution for comparison with the Lyra solution in the x,z frame. Lyra's calculations extend from the ground up

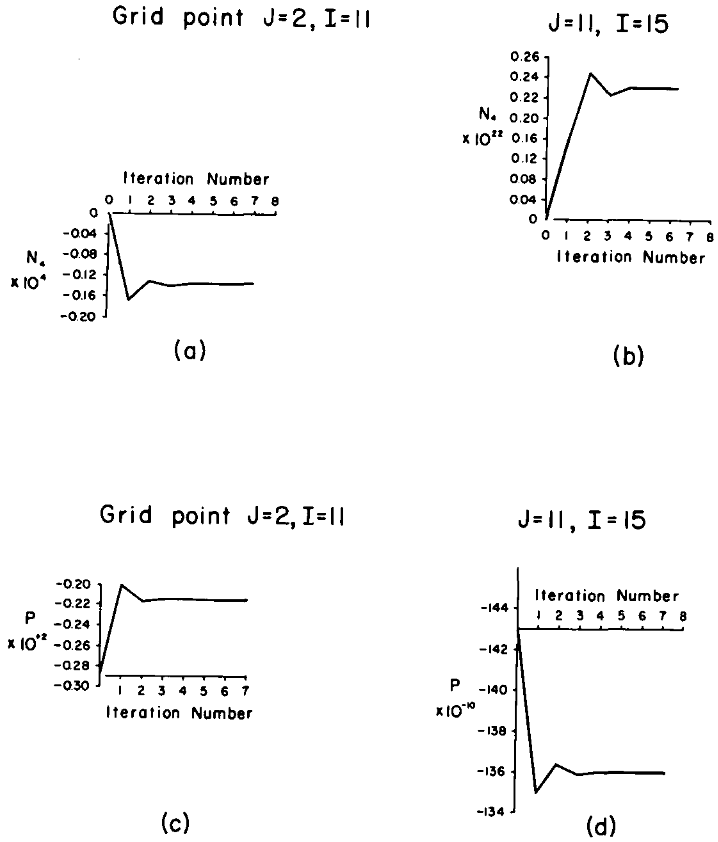

FIGURE 8.—The slope of the streamline P, and the nonlinear term of the wave equation N_4, plotted as a function of the iteration number at two selected grid points. Illustrates convergence of nonlinear iteration.

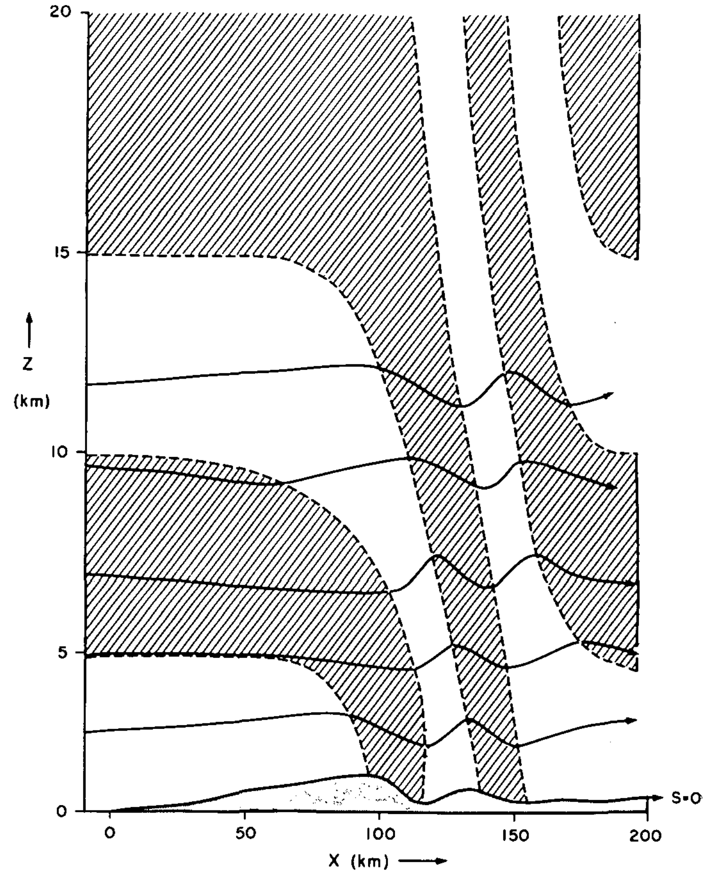

FIGURE 9.—Streamlines and their slopes (hatched) for air flow over Sierras. (Isothermal atmosphere, no shear, $\overline{T}=250°$A., $\overline{U}=$ 20 m.p.s.)

to a height of approximately 10 km. Our vertical grid distance $\Delta s=200$ gives a very coarse resolution. This corresponds to $\Delta z\approx 5$ km. and hence the comparison cannot be very good. The sloping trough and ridge lines are very well described with waves of approximately 10-km. wavelength. It is however promising to see that the numerical program yields solutions very close to what we intuitively expected to find.

In figure 9 we present the results of air flow over the Sierra profile for an isothermal atmosphere with no vertical wind shear. The results are projected on the x,z coordinates. The sloping dashed lines separate regions of $P>0$ from regions $P<0$ (shaded). The grid distances and the constants are the same as in the previous example.

The results bear strong similarity to those obtained by Queney [12] for a bell-shaped mountain in an isothermal, no shear atmosphere. The sloping lines $P=0$ have an upwind tilt. The amplitudes of the schematic streamlines in the upper part are exaggerated. The strong foehn wind effect over the Owens valley ($x\approx 120$ km.) is very clearly shown by the shaded region of sinking air.

Calculations of this kind seem to be most interesting from the standpoint of the numerical approach. This calculation is an extension of the type of numerical work suggested by Wallington [18]. Here we have a continuous mountain profile described by a very large number of grid points. As in the previous example the nonlinear effects were found to be small. It is interesting to notice the following other features:

(i) Wavelength$\approx$40 km.

(ii) On the upwind side there are several interesting alternating modes: a rising mode below 5 km., a sinking mode between 5 and 10 km., and again a rising mode.

Examination of individual soundings to determine the flow over the Sierras during varying wind and thermal stability conditions would be of natural interest. This kind of calculation can be performed through this numerical program.

EXAMPLES WITH VARYING STABILITY AND SHEAR

It would be of considerable interest to compare the numerical calculations with the analytic results for various two- and three-level models based on Scorer's [15] work. In view of the differences in the upper boundary condition at $s=s_\infty$ an exact comparison is not possible.

We shall present two examples of flow over the Sierras with typical mean soundings during summer and spring.

In their analysis of a many-layered atmosphere Eliassen and Palm [5] discussed the role of the reflection coefficient in several layers. The coefficient determines whether the solution of the linear wave equation would be trigonometric or exponential in any layer.

The corresponding analysis is presented in the x, s frame

$$F_1\frac{\partial^2 P}{\partial x^2}+F_2\frac{\partial P}{\partial s}+F_3\frac{\partial^2 P}{\partial s^2}+F_4P=0$$

Let

$$P^{(1)}=e^{1/2\int F_2/F_3 ds}P$$

and

$$\nabla_s^2=\frac{F_1}{F_3}\frac{\partial^2}{\partial x^2}+\frac{\partial^2}{\partial s^2}$$

We obtain the canonical form

$$\nabla^2P^{(1)}+\left[\frac{F_4}{F_3}-\left(\frac{F_2^2}{4F_3^2}+\frac{1}{2}\frac{\partial}{\partial s}\frac{F_2}{F_3}\right)\right]P^{(1)}=0 \tag{47}$$

In equation (47) we may write

$$G=\frac{F_4}{F_3}-\left(\frac{F_2^2}{4F_3^2}+\frac{1}{2}\frac{\partial}{\partial s}\frac{F_2}{F_3}\right)$$

If we separate variables by assuming $P^{(1)}$ to be made the product of two functions of x and s, then the condition for vertical propagation of a horizontal wave number κ may be obtained by conventional techniques.

If $(G-\kappa^2)<0$ Vertical solution is exponential.

$(G-\kappa^2)>0$ Vertical solution is trigonometric.

It may be pointed out here (in the context of equation (47)) that no upward propagation of energy is possible if the wave solutions are of exponential type (Eliassen and Palm [5]).

Thus a vertical plot of G as a function of s would determine whether a horizontal wave number κ is propagated upward as a wave or not.

Figure 10 shows a plot of G during different seasons and for the isothermal atmosphere. For the latter, G is a constant and has a value of $\approx 6\times10^{-4}$. Along the abscissa we have indicated a wavelength scale that determines in length units ($\lambda=2\pi/\kappa$) the propagation of a wave number κ. It is easy to see that the isothermal atmosphere would permit vertical propagation of wavelength greater than a few kilometers all the way to the top. The individual soundings of G show the possibility of trapping of energy. Values of G during spring and for the sounding taken from a paper by Palm and Foldvik [11] show rather large values in the lower stratosphere. This analysis is analogous to that of Charney and Drazin [3] for long atmospheric waves.

The numerical solution for $(P=\partial z/\partial x)_s$ would thus exhibit waves of certain wave number κ if $G>\kappa^2$. The mean soundings during summer and spring are illustrated

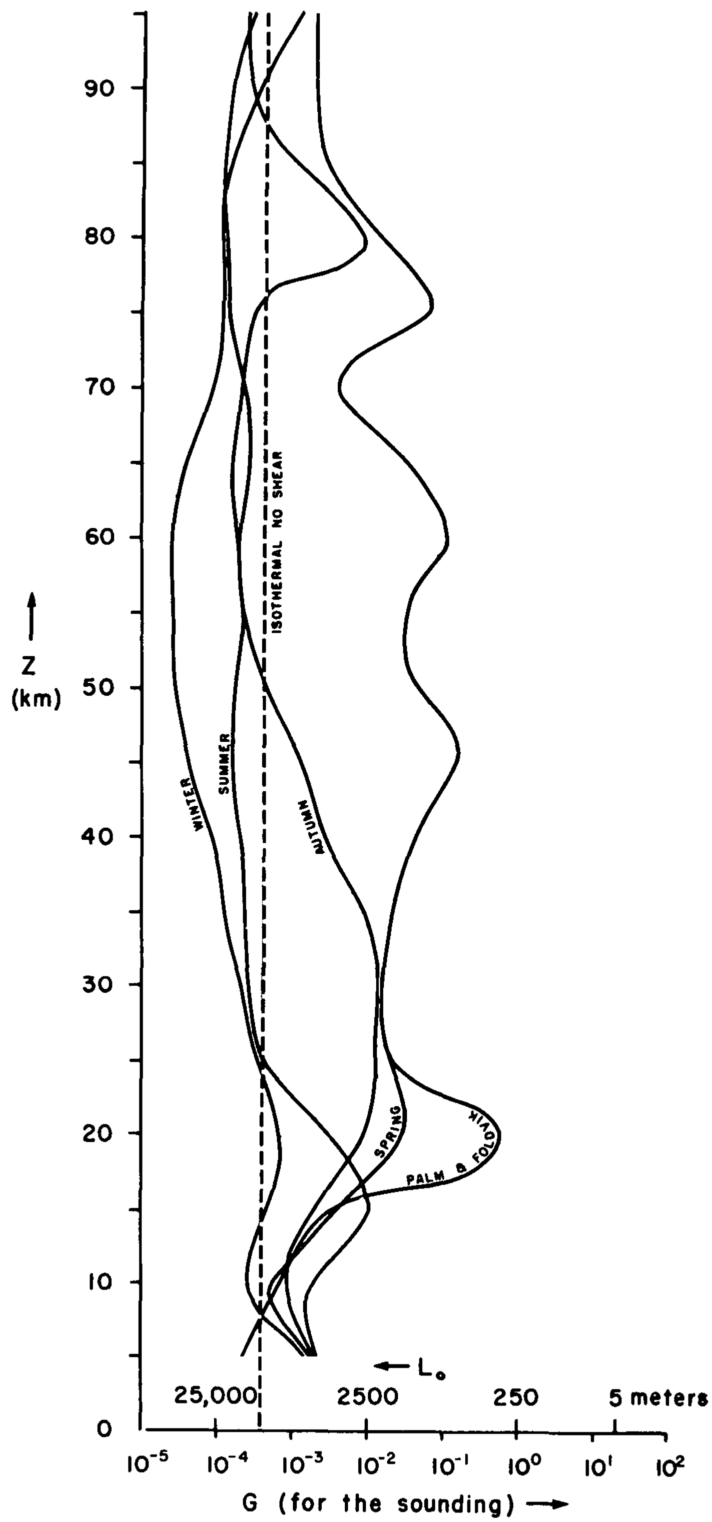

FIGURE 10.—The refractive index of the medium, G, is plotted as a function of height z during different seasons (to 100 km.) and for Palm and Foldvik [11] sounding (to 20 km.). The horizontal scale is also represented as a function of the wavelength.

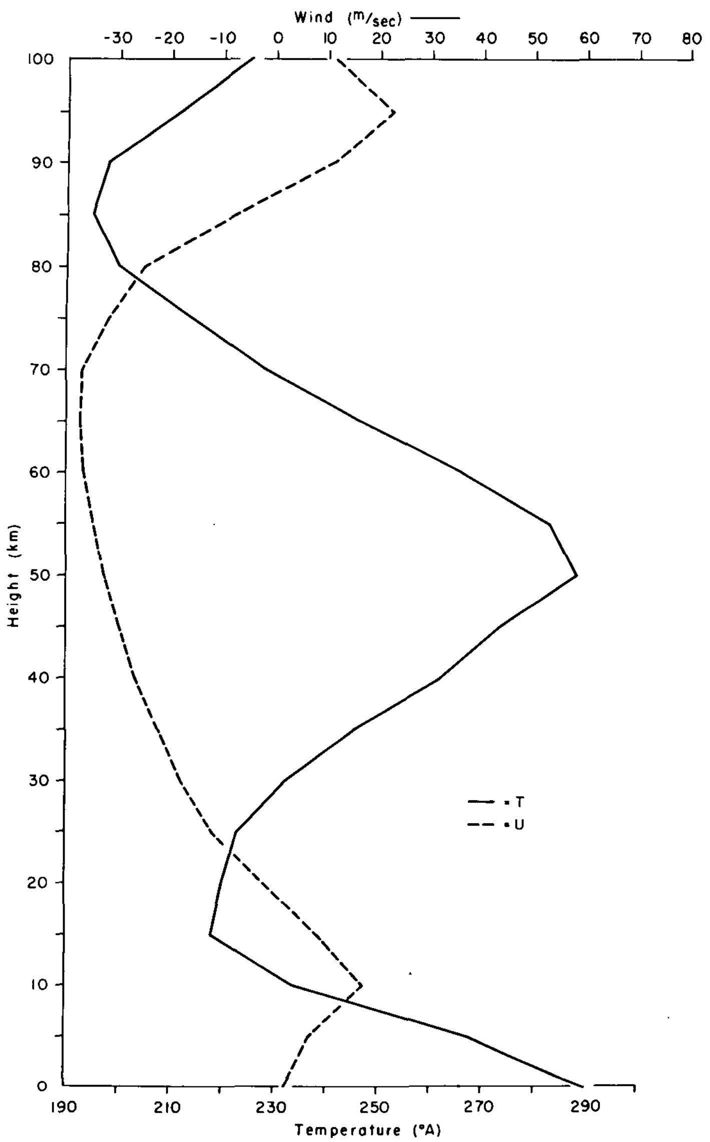

FIGURE 11.—Vertical distribution of temperature T and zonal wind U, during summer.

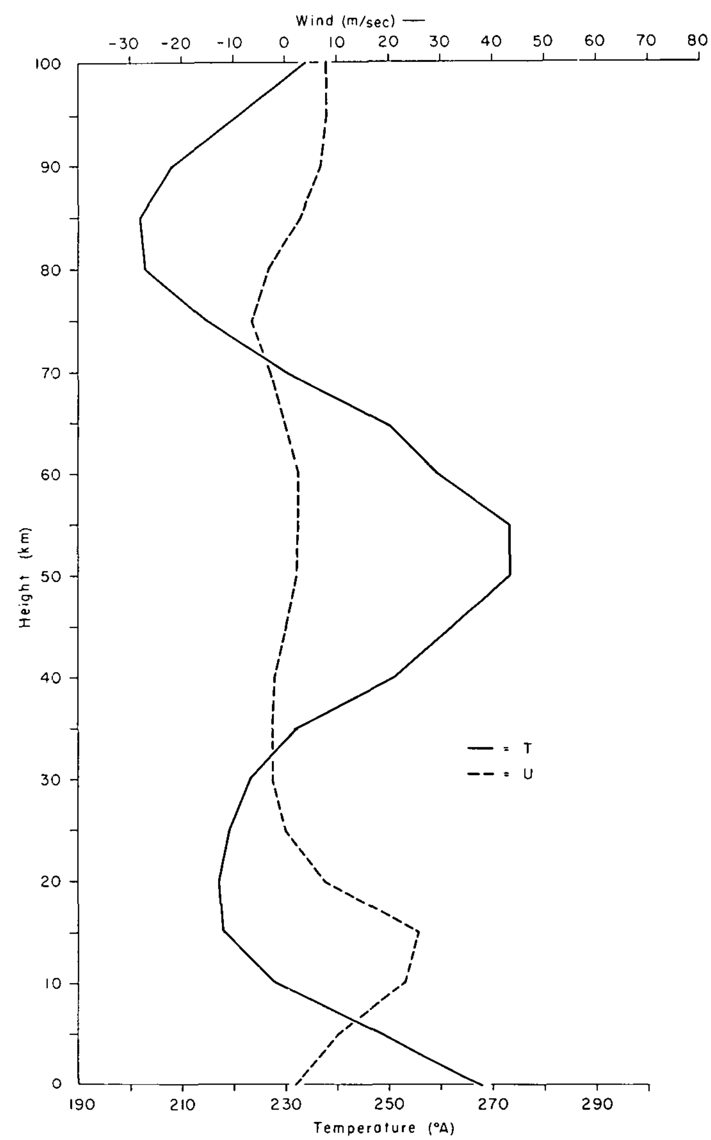

FIGURE 12.—Vertical distribution of temperature T, and zonal wind U, during spring.

in figures 11 and 12. These were obtained from a report by Batten [1]. This represents the mean wind and temperature between 30° and 40° N. from a large number of United States rocket observations. We assume that a mean atmosphere described by these soundings constitutes the unperturbed flow over the complete Sierra profile. From figure 10 we find that G values for summer are much smaller than those of spring. We would thus expect vertical propagation of shorter gravity waves in spring than in summer. The Sierra profile may be expected to excite an infinite spectrum of these wave numbers. Figures 13 and 14 show respectively the solution for summer and spring. The two solutions exhibit large differences in scale as expected. A rather large vertical damping shows up around 40 km. in spring; this solution is characterised by short gravity waves, with a horizontal wavelength of approximately 20 km. The summer solution, except for the lower troposphere, does not seem to exhibit these typical mountain wave characteristics. Energy in low wave numbers seems to propagate to great heights in summer. It may be noted that during summer a part of the marching calculations are carried out against the current (the stratospheric easterlies). This does not violate any conditions on the uniqueness. In this case we still obtain a unique downstream set of numbers P^* that calls for no wave to the left of the Sierras. In reality, perhaps the tropospheric westerlies in summer would contain a spectrum of mountain waves; these waves if carried up would carry energy westward in the stratospheric easterlies. Our choice of boundary conditions would not show this mode in the stratosphere, hence the solution shown in figure 13 may be of interest only in the troposphere.

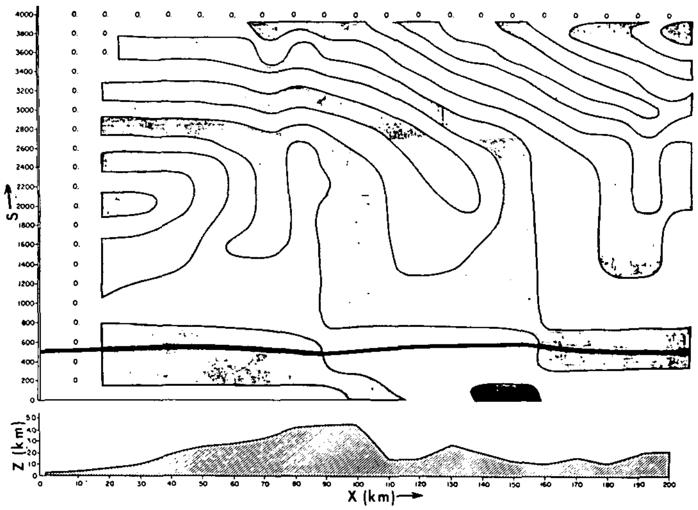

FIGURE 13.—Nonlinear solution for air flow over Sierras during summer. Rest same as in figure 5.

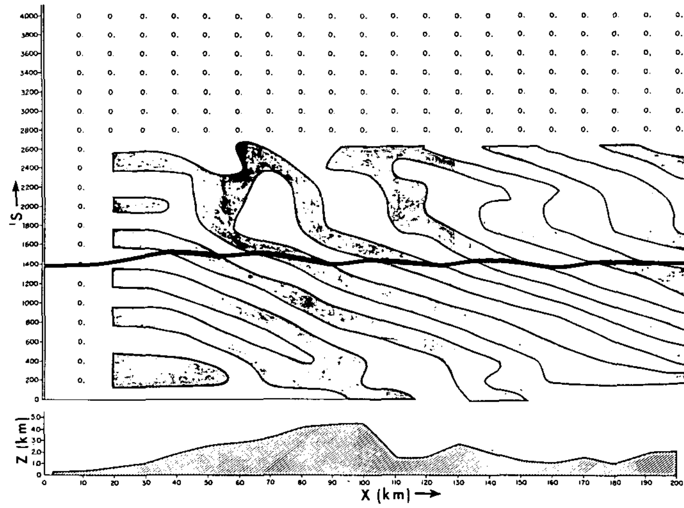

FIGURE 14.—Nonlinear solution for air flow over Sierras during spring. (The zeros on the top refer to slope of streamlines less than 10^{-30}.) Rest same as in figure 5.

The spring values of G are large and close to those obtained by Palm and Foldvik [11], for a case of large mountain wave activity near Leuchars. The nonlinear numerical solution for P, figure 14, is very similar to the linear analytic solution of Palm and Foldvik. The horizontal and vertical scales of the waves appear to be very realistic. The large damping of P in this case suggested that the locale of the upper boundary condition was less restricted. We had chosen $s_\infty=4000$; however the solution would be identical had s_∞ been any value greater than 2800.

9. CONCLUDING REMARKS

We have formulated the two-dimensional mountain wave problem in isentropic coordinates. The analytical representation of the problem in this coordinate is shown to have certain advantages over the conventional height coordinates.

The numerical marching scheme can be utilized to obtain solutions for mountains of any arbitrary shape. Even though the theory of the computational stability criterion is not completely understood, we can, however, say that the numerical solution is unique in that it satisfies the Kelvin monotony condition. This has enabled us to extend this work to obtain solutions for mountain waves in a medium with varying conditions of shear and stability. The solutions appear very realistic when we compare with those obtained by Lyra and Queney. The vertical resolution in the numerical marching scheme is very coarse ($\Delta s=200$ c.g.s. units); this corresponds to a Δz approximately 5 km. A finer vertical resolution would be required in the treatment of problems of airflow in an atmosphere where sharp changes in the reflection coefficient are present. The computation time on IBM 7090 type of computer for some of these calculations presented here is of the order of 20 min. A finer vertical resolution would make the computer time longer because a much smaller space-step, Δx, would be needed for a computationally stable marching scheme.

Some calculations for individual wintertime soundings over the Sierras did not yield convergence of the numerical solution. These were cases where very large changes in the reflection coefficient G were observed. The computational stability criterion depends on the magnitude of G; these failures of the computations are thus attributable to this property of the medium. A vertical smoothing of the G function enabled us to obtain convergence in some cases.

The problem of vertical propagation of energy by mountain waves was discussed briefly in the Introduction. The numerical solutions show that a large amount of mountain wave energy is propagated into the stratosphere, in some instances to very great heights. Further work in this area needs to be done to explain the ionospheric turbulence phenomena and the presence of noctilucent clouds. One of the difficulties in pursuing this kind of work stems from the lack of a clear description of the structure of the medium to great heights. Also, it is not always possible to isolate an individual hill or mountain as the energy source.

It may be worth mentioning here that, Makjanic [9] utilized the isentropic coordinate to obtain a linear fourth-order differential equation to discuss mountain waves in a medium with Navier-Stokes type of friction. He could not formally solve this system for any particular mountain profile like that used by Queney, because of complexities in the mathematics. He utilised an analytic procedure and obtained a frequency equation for waves. Since no solutions were obtained it is not possible to evaluate his work, except perhaps to state that numerical work of the kind we have pursued here may be of help in examining problems with friction.

At the time of writing their report, Queney et al. [13] stated that no initial value lee-wave problems have been solved by a numerical procedure. Adiabatic models of this kind can be examined by numerical methods and would be extensions of the work presented here.

ACKNOWLEDGMENTS

This work was supported by grants NSF G-18048 and NSF 13575. The author acknowledges the sponsorship of the project directors, Professor J. Bjerknes and Professor G. F. MacDonald. I have greatly benefited from several discussions with Dr. Barislav Makjanic and Professor Jorgen Holmboe.

REFERENCES

1. E. S. Batten, "Wind Systems in the Mesosphere and Lower Ionosphere," *Journal of Meteorology*, vol. 18, No. 3, June 1961, pp. 283–291.
2. V. Bjerknes et al., *Physikalische Hydrodynamik*, J. Springer Verlag., Berlin, 1933, 797 pp.
3. J. G. Charney and P. G. Drazin, "Propagation of Planetary-Scale Disturbances from the Lower into the Upper Atmosphere," *Journal of Geophysical Research*, vol. 66, No. 1, Jan. 1961, pp. 83–109.
4. G. A. Corby and J. S. Sawyer, "The Airflow over a Ridge: The Effects of the Upper Boundary and High Level Conditions," *Quarterly Journal of the Royal Meteorological Society*, vol. 84, No. 359, Jan. 1958, pp. 25–37.
5. A. Eliassen and E. Palm, "On Transfer of Energy in Stationary Mountain Waves," *Geofysiske Publikasjoner*, vol. 22, No. 3, Sept. 1961, pp. 1–36.
6. C. O. Hines, "The Upper Atmosphere in Motion," *Quarterly Journal of the Royal Meteorological Society*, vol. 89, No. 379, Jan. 1963, pp. 1–42.
7. Lord Kelvin (William Thompson), "On Stationary Waves in Flowing Water," *Philosophical Magazine*, vol. 5, 1886, pp. 353–357, 445–452, 517–530.
8. G. Lyra, "Über den Einfluss von Bodenerhebungen auf die Strömung einer stabil geschichteten Atmosphäre," *Beiträge zur Physik der freien Atmosphäre*, Band 26, 1940, pp. 197–206.
9. B. Makjanic, "A Contribution to the Mathematical Theory of Air Flow over Mountains Including Effects of Turbulent Viscosity," Department of Meteorology, University of California, 1962 (Unpublished Technical Report).
10. P. M. Morse and H. Fishbach, *Methods of Theoretical Physics*, vol. II, McGraw-Hill Book Co., Inc., New York, 1953.
11. E. Palm and A. Foldvik, "Contribution to the Theory of Tow-Dimensional Mountain Waves," *Geofysiske Publikasjoner, Geophysica Norvegica*, vol. 21, No. 6, Mar. 1960, 30 pp.
12. P. Queney, "Theory of Perturbations in Stratified Currents with Application to Airflow over Mountain Barriers," *Miscellaneous Reports*, No. 23, The University of Chicago, 1947, 81 pp.
13. P. Queney et al., "The Air Flow over Mountains," *Technical Report* No. 34, World Meteorological Organization, Geneva, 1960, 135 pp.
14. Lord Rayleigh (J. W. Strutt), "The Form of Standing Waves on the Surface of Running Water," *Proceedings, London Mathematical Society*, vol. 15, 1883, pp. 69–78.
15. R. S. Scorer, "Theory of Waves in the Lee of Mountains," *Quarterly Journal of the Royal Meteorological Society*, vol. 75, No. 323, Jan. 1949, pp. 41–56.
16. A Sommerfeld, "Die Greensche Funktion der Schwingungsgleichung," *Jahresberichte*, Deutsche Mathematiker-Vereinigung, vol. 21, 1912, pp. 309–353.
17. A. Sommerfeld, *Vorlesungen über theoretische Physik*, vol. VI, Akademische Verlagsgesellschaft, Leipzig, 2d rev. ed., 1948, p. 191.
18. C. E. Wallington, "A Numerical Study of the Topographical Factor in Lee-Wave Amplitudes," *Quarterly Journal of the Royal Meteorological Society*, vol. 84, No. 362, Oct. 1958, pp. 428–433.
19. M. G. Wurtele, "The Initial-Value Lee-Wave Problem for the Isothermal Atmosphere," Scientific Report No. 3, Sierra Wave Project, under Contract No. AF 19(122)–263, Department of Meteorology, University of California, Los Angeles, 1953.
20. J. Zierep, "Neue Forschungsergebnisse aus dem Gebiet der atmosphärischen Hinderniswellen," *Beiträge zur Physik der Atmosphäre*, vol. 29, No. 3, 1957, pp. 143–153.

[*Received August 1, 1963; revised November 18, 1963*]